AJNR

Cerebral Hemodynamic and Metabolic Abnormalities in Neonatal Hypocalcemia: Findings from Advanced MRI

Ying Qi, Zixuan Lin, Hanzhang Lu, Jian Mao, Hongyang Zhang, Pengfei Zhao and Yang Hou

AJNR Am J Neuroradiol published online 14 September 2023
http://www.ajnr.org/content/early/2023/09/14/ajnr.A7994

Published September 14, 2023 as 10.3174/ajnr.A7994

ORIGINAL RESEARCH
PEDIATRICS

Cerebral Hemodynamic and Metabolic Abnormalities in Neonatal Hypocalcemia: Findings from Advanced MRI

Ying Qi, Zixuan Lin, Hanzhang Lu, Jian Mao, Hongyang Zhang, Pengfei Zhao, and Yang Hou

ABSTRACT

BACKGROUND AND PURPOSE: Neonatal hypocalcemia is the most common metabolic disorder, and whether asymptomatic disease should be treated with calcium supplements remains controversial. We aimed to quantify neonatal hypocalcemia's global CBF and cerebral metabolic rate of oxygen ($CMRO_2$) using physiologic MR imaging and elucidate the pathophysiologic vulnerabilities of neonatal hypocalcemia.

MATERIALS AND METHODS: A total of 37 consecutive patients with neonatal hypocalcemia were enrolled. They were further divided into subgroups with and without structural MR imaging abnormalities, denoted as neonatal hypocalcemia-a ($n = 24$) and neonatal hypocalcemia-n ($n = 13$). Nineteen healthy neonates were enrolled as a control group. Brain physiologic parameters determined using phase-contrast MR imaging, T2-relaxation-under-spin-tagging MR imaging, and brain volume were compared between patients with neonatal hypocalcemia (their subgroups) and controls. Predictors for neonatal hypocalcemia–related brain injuries were identified using multivariate logistic regression analysis and expressed as ORs with 95% CIs.

RESULTS: Patients with neonatal hypocalcemia showed significantly lower CBF and $CMRO_2$ compared with controls. Furthermore, the neonatal hypocalcemia-a subset (versus controls or neonatal hypocalcemia-n) had significantly lower CBF and $CMRO_2$. There was no obvious difference in CBF and $CMRO_2$ between the neonatal hypocalcemia-n subset and controls. CBF and $CMRO_2$ were independently associated with neonatal hypocalcemia. The ORs were 0.80 (95% CI, 0.65–0.99) and 0.97 (95% CI, 0.89–1.05) for CBF and $CMRO_2$, respectively.

CONCLUSIONS: Neonatal hypocalcemia with structural damage may exhibit lower hemodynamics and cerebral metabolism. CBF may be useful in assessing the need for calcium supplementation in asymptomatic neonatal hypocalcemia to prevent brain injury.

ABBREVIATIONS: AUC = area under the curve; $CMRO_2$ = cerebral metabolic rate of oxygen; iCa = ionized calcium; NHC = neonatal hypocalcemia; NRDS = neonatal respiratory distress syndrome; PCMR = phase-contrast MR imaging; PVWM = periventricular WM; TRUST = T2-relaxation-under-spin-tagging; Yv = venous oxygenation

Neonatal hypocalcemia (NHC) is a common abnormality in neonates.[1] Prematurity, perinatal asphyxia, sepsis, maternal vitamin D deficiency, diabetes, hypoparathyroidism, and hypomagnesemia are the most common causes of NHC.[2-5] Early- and late-onset NHC occurs before and after the first 3 days of life, respectively. The clinical presentation of NHC is frequently asymptomatic but can be symptomatic, showing neuromuscular irritability, such as myoclonic jerks, jitteriness, exaggerated startles, and seizures. NHC can be life-threatening[6] and is a risk factor for mortality in critically ill infants.[7] NHC can be prevented or treated with long-term calcium gluconate therapy specific to its etiology. However, calcium supplementation should be administered carefully in patients with hypoxic-ischemic encephalopathy. Hypoxia causes a rapid influx of calcium into cells, resulting in apoptosis, while calcium supplementation can aggravate brain damage in these patients.[5] In addition, whether asymptomatic NHC should be treated with calcium supplementation is controversial because it may cause neonatal tetany or seizures.[1]

Received June 12, 2023; accepted after revision August 16.

From the Departments of Radiology (Y.Q., H.Z., Y.H.) and Pediatrics (J.M.), Shengjing Hospital of China Medical University, Shenyang, China; Key Laboratory for Biomedical Engineering of Ministry of Education (Z.L.), Department of Biomedical Engineering, College of Biomedical Engineering & Instrument Science, Zhejiang University, Hangzhou, China; Department of Radiology (H.L.), Johns Hopkins University School of Medicine, Baltimore, Maryland; and Department of Pharmacology (P.Z.), School of Pharmaceutical Sciences, China Medical University, Shenyang, China.

This study was supported by the Applied Basic Research Project of Liaoning (2022JH2/101500061), the Medical Education Research Project of Liaoning (No.2022-N006-01), the New Technology Project of Shengjing Hospital, and the 345 Talent Project of Shengjing Hospital of China Medical University.

Pengfei Zhao, and Yang Hou contributed equally to this work.

Please address correspondence to Yang Hou, PhD, 36# of Sanhao St, Heping District, Shenyang, China; e-mail: houyang1973@163.com

Indicates article with online supplemental data.

http://dx.doi.org/10.3174/ajnr.A7994

Table 1: Demographic and clinical data of the NHC group and controls

	NHC ($n = 37$)	NHC-a ($n = 24$)	NHC-n ($n = 13$)	Control ($n = 19$)	$P_{NHC\ \&\ Control}$ Value
Demographics					
Males (No.) (%)	24 (64.9)	14 (58.3)	7 (53.8)	14 (73.7)	.11
Birth weight (mean) (g)	2024.9 (SD, 614.5)	2080.8 (SD, 532.1)	1676.5 (SD, 695.9)	2434.7 (SD, 1047.5)	.13
Scan age (mean) (wk)	37.0 (SD, 2.9)	37.2 (SD, 3.2)	36.0 (SD, 1.8)	37.0 (SD, 4.0)	.99
Clinical					
Apgar score (mean)					
1 min	7.6 (SD, 3.2)	7.0 (SD, 3.5)	9.4 (SD, 0.5)	9.6 (SD, 0.8)	<.05
5 min	6.2 (SD, 3.3)	5.5 (SD, 3.5)	8.0 (SD, 1.3)	8.6 (SD, 2.1)	<.05
NRDS (No.) (%)	16 (43.2)	13 (54.2)	3 (23.1)	–	–
Twins (No.) (%)	6 (16.2)	5 (20.8)	1 (7.7)	–	–
iCa (mean) (mmol/L)	0.9 (SD, 0.2)	0.9 (SD, 0.2)	0.8 (SD, 0.1)	1.2 (SD, 0.1)	<.05

Note:—The en dash indicates none.

Therefore, gaining a better understanding of the neurobiologic characteristics of NHC and its relationship with serum calcium levels may provide important insights into neonatal pathophysiologic vulnerabilities.

CT perfusion,[8,9] ^{15}O-PET,[10] ^{133}Xe-enhanced CT,[11] DSC MR imaging,[12] and near-infrared spectroscopy[13] are common methods of measuring the hemodynamics and metabolism in the neonatal brain but require ionizing radiation and exogenous tracers, which can cause kidney injury and may create motion artifacts or low spatial resolution. Doppler sonography is used to evaluate brain perfusion but does not allow whole-brain perfusion analyses and is not always reproducible, especially when performed by less-experienced neonatal operators.[14] Recent advances in MR imaging technologies allow noninvasive and quantitative measurements of brain hemodynamic parameters without the need for contrast material injection or exposure to ionizing radiation. Global CBF can be measured using arterial spin-labeling[15] and phase-contrast MR imaging (PCMR).[16] CBF measurements using arterial spin-labeling agree with those of ^{15}O-PET and DSC MR imaging.[17,18] However, low CBF and neonatal brain volume reduce the accuracy of arterial spin-labeling quantitative measurement, especially in deep white matter.[19] PCMR has been successfully reported in neonates and requires <2 minutes.[20] Venous oxygenation (Yv) of the brain can be determined using the T2-relaxation-under-spin-tagging (TRUST) MR imaging technique. Yv and CBF can be combined to assess the global cerebral metabolic rate of oxygen ($CMRO_2$).[21,22] All these physiologic measurements require <5 minutes, which is suitable for the neonatal population. Most neonatal studies have focused on low birth weight,[23] brain injury such as hypoxic-ischemic encephalopathy detected with near-infrared spectroscopy,[24] and WM lesions detected with PCMR and TRUST MR imaging.[20] Few perinatal studies have been conducted on the effects of NHC on cerebral oxygen metabolism and hemodynamics.

The present study aimed to comprehend the relationship among NHC, its hemodynamics, and cerebral oxygen metabolism using PCMR and TRUST MR imaging for a better understanding of its pathophysiologic process and improvement of treatment.

MATERIALS AND METHODS

Ethics Statement

The study protocol was approved by the Ethics Committee of the Shengjing Hospital of China Medical University (IRB2021PS094K). Written informed consent was waived because the data were collected as part of a clinically indicated MR imaging. None of the authors has any conflict of interest to declare. Agreement to be accountable for all aspects of the work in ensuring that questions related to the accuracy or integrity of any part of the work are appropriately investigated and resolved.

Participants and Study Design

Between June 2021 and April 2022, fifty-six neonates were enrolled. The participants were categorized into the NHC and control groups. The inclusion criteria for the NHC group were asymptomatic neonates with early-onset NHC occurring in the first 3 days of life. Participants were further divided into those with abnormal MR imaging findings, denoted as NHC-a, and those with normal MR imaging findings, denoted as NHC-n. NHC is defined as ionized calcium (iCa) <4 mg/dL (1 mmol/L) in preterm infants and <1.2 mmol/L in term neonates.

The inclusion criteria for the control group were asymptomatic neonates without NHC and abnormal MR imaging findings or laboratory results at birth. They had normal results from umbilical cord blood gas analysis, the liver function test, routine blood examination, and serum and ion analyses at birth. The purpose of MR images was for exclusions of abnormalities of the nervous system. The exclusion criteria were congenital malformations, severe infection, major congenital heart disease, and unusable MR images. Neonates' demographic and clinical data are summarized in Table 1. Detailed information is provided in the Online Supplemental Data (There were 27 cases [sodium levels <135 mmol/L] of hypocalcemia with low serum sodium, including 11 cases with sodium levels of <130 mmol/L [range, NHC-n, 123.4–145.6 mmol/L versus NHC-a, 121.9–144.0 mmol/L]). Two experienced neuroradiologists (Y.Q. and X.X.Q., each with 12 years of experience and blinded to the group data) diagnosed and graded the injuries on MR imaging as described on a scale of I–IV, according to their size, number, and distribution, as summarized in previous Table 1 reported by Childs et al.[25]

MR Imaging Protocol

Imaging was performed on a 3T scanner (Ingenia; Philips Healthcare) without sedation. Axial T1WI and T2WI were acquired using the following settings: TR, 200/5000 ms; TE, 2.3/80 ms;

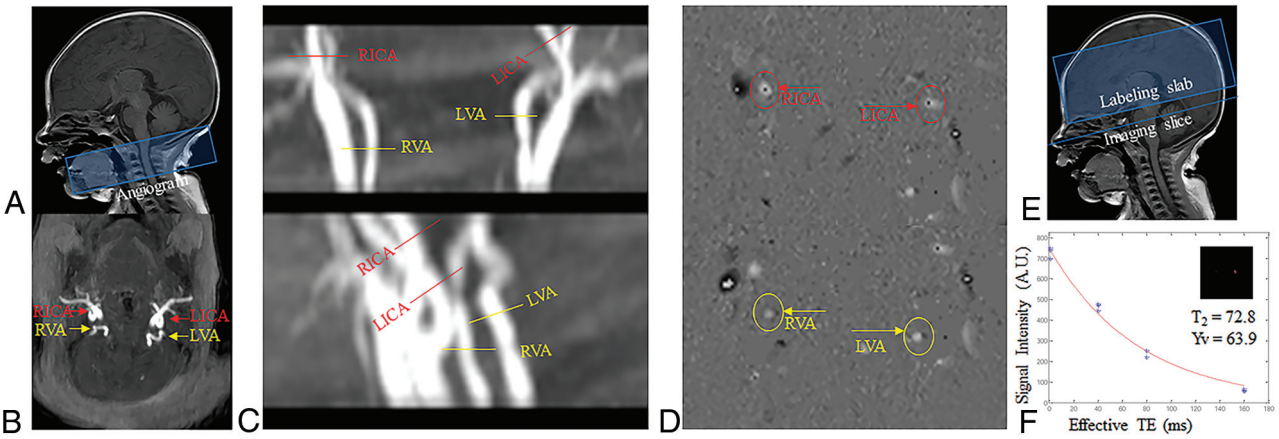

FIG 1. Sample images for CBF and Yv determination. *A*, Positioning of the imaging section. *B* and *C*, PCMR imaging section locations for the LICA, RICA, LVA, and RVA on the MIP image of a TOF angiogram. *D*, The manual delineation of LICA, RICA, LVA, and RVA was conducted to determine flux in these vessels. The sum of fluxes by brain weight yielded the CBF. *E*, The imaging section was positioned parallel to the intercommissural line with a 10-mm distance from the superior sagittal sinus (SSS). TRUST MR imaging used a spin-labeling module to isolate pure venous blood signals in the SSS. *F*, Blood signals from the SSS were fitted to a monoexponential function of the effective TE to yield blood T2. T2 was converted to Yv via a calibration plot. LICA indicates left internal carotid arteries; RICA, right internal carotid arteries; LVA, left vertebral artery; RVA, right vertebral artery; AU, arbitrary unit.

section thickness, 5/5 mm; FOV, 180 × 150 × 90 mm^3; matrix size, 224 × 162/112 × 112; scan time, 34.4/40.9 seconds.

CBF Determination

First, TOF MRA was performed to visualize the left and right ICAs and vertebral arteries. The imaging slab was positioned at the center of the epistropheus, with 60-mm saturation slabs placed above to suppress venous signals. Second, PCMR used bipolar gradients to encode flow velocity in the major feeding arteries, thereby providing a measurement of CBF. PCMR settings were the following: single section; voxel size, 0.5 × 0.5 × 3 mm^3; FOV, 180 × 180 × 3 mm^3; maximum velocity encoding, 20 cm/s; and total scan time, 1.5 minutes. Manual delineation of the arterial ROI was performed on the magnitude image of each PCMR scan and then applied to the velocity maps to obtain the flux in all vessels, the sum of which yielded the total blood flow (milliliters/minute). To convert the value to CBF, we obtained brain volume by manual tracing of the T2WI and assuming a parenchymal density of 1.06 g/mL.[26] CBF was calculated by dividing the total flux by the brain weight (Fig 1*A*–*D*).

Arterial and Venous Oxygenation Determination

Arterial oxygenation was measured using a pulse oximeter in the right hand. Yv was measured by TRUST MR imaging with the following settings: 4 effective TEs, 0, 40, 80, and 160 ms; TR, 3000 ms; TI, 1022 ms; FOV, 160 × 160 × 5 mm^3; matrix size, 64 × 61; sensitivity encoding factor, 3; voxel size, 2.5 × 2.5 × 5 mm^3; thermal Carr-Purcell-Meiboom-Gill (τCPMG), 10 ms; scan time, 72 seconds.[20] TRUST MR imaging applies a spin-labeling module to isolate pure venous blood signals, a series of T2-preparation pulses to modulate the MR imaging signal, and uses monoexponential fitting to yield blood T2, which was converted to Yv using a hematocrit-specific T2-Yv calibration curve. Data processing for PCMR and TRUST MR imaging was performed as previously described (Fig 1*E*, *-F*).[16,20,22]

$CMRO_2$ Calculation

$CMRO_2$ can be calculated using the Fick principle,[26] in which HCT is hematocrit.

$$CMRO_2 = CBF \times (Ya - Yv) \times \frac{HCT \times 897}{44\%}.$$

Statistical Analysis

To compare baseline demographics, clinical characteristics, and physiologic parameters among the 3 groups, we used a Student *t* test or Wilcoxon 2-sample exact test (for continuous variables) and a χ^2 test (for categoric variables). To evaluate group differences with respect to scan age, birth weight. and twins, multiple linear regressions were examined to predict the measured physiologic parameters (Yv, CBF, and $CMRO_2$) and brain volume that can be influenced by NHC using 4 operating input parameters: group (NHC-a, NHC-n, or controls), neonatal scan age, birth weight, and twins. Similar analyses were performed to examine the dependence of physiologic parameters and brain volume on iCa levels. Physiologic parameters and brain volume were assigned as dependent variables, whereas the brain iCa level, scan age, birth weight, and twins were assigned as independent variables. Considering the effects of gestational age, birth weight, Apgar score, sex, and blood gas analysis on structural abnormalities, we used univariate and multivariate logistic regression analysis, respectively. The risk factors for predicting NHC with structural MR imaging abnormalities were identified using multivariate logistic regression analysis expressed as ORs with 95% CIs. Receiver operating characteristic curves were used to determine whether physiologic parameters, iCa levels, scan age, birth weight, or the incorporation of above values together (physiological parameters + iCa levels + scan age + birth weight) could facilitate the diagnosis of neonatal brain injuries and to identify the cutoff points for risk factors associated with neonatal brain injuries. All computations were performed using standard software (SPSS; IBM). $P < .05$ indicates a statistically significant difference.

RESULTS

Participant Characteristics

Figure 2 shows a schematic of participant selection. Neonates' MR imaging findings, focal periventricular WM (PVWM) lesion grades, and their physiologic parameters are summarized in Table 2. Figure 3 shows MR imaging findings of representative neonates in the NHC-a subgroup with different severities. The physiologic parameters of the participants in the NHC and control groups are shown in Table 3. The NHC neonates and the NHC-a subset (versus controls) had significantly lower CBF ($P = .03$, $P = .001$) and $CMRO_2$ ($P = .02$, $P = .002$). CBF and $CMRO_2$ proved significantly lower in the NHC-a (than in the NHC-n) subset ($P = .001$, $P = .01$). There were no significant differences in CBF and $CMRO_2$ between the NHC-n subset and controls ($P = .70$, $P = .63$). Yv and brain volume were not significantly different among groups ($P > .05$). Figure 4 shows Yv, CBF, $CMRO_2$, and brain volume in both groups and subgroups using boxplots. There were 5 neonates with SAH not secondary to parenchymal bleeding primarily from the germinal matrix. Only 1 neonate with neonatal respiratory distress syndrome (NRDS) in grade III diagnosed by x-ray in our study required a surfactant within 2 hours after birth.

Linear Regression Analysis of Measured Physiologic Parameters Associated with Group (NHC-a, NHC-n, or Control Groups), Scan Age, Birth Weight. and Twins

The multilinear regression analysis showed that CBF and $CMRO_2$ were significantly correlated with group ($\beta = -2.6$, $P = .001$; $\beta = -6.5$, $P = .001$, respectively). Yv and brain volume had a nonsignificant relationship with category ($\beta = 0.7$, $P = .69$; $\beta = 13.1$, $P = .20$). Yv, $CMRO_2$, and brain volume had a significant relationship with scan age ($\beta = -1.2$, $P = .03$; $\beta = 1.3$, $P = .03$; $\beta = 14.5$, $P < .001$). CBF was nonsignificantly correlated with scan age ($\beta = 0.4$, $P = .07$). Yv was significantly correlated with birth weight ($\beta = 0.006$, $P = .01$). CBF, $CMRO_2$, and brain volume were nonsignificantly correlated with birth weight ($\beta = 0.001$, $P = .53$; $\beta = 0.003$, $P = .30$; $\beta = 0.008$, $P = .55$, respectively). Yv, CBF, and $CMRO_2$ were nonsignificantly correlated with twins ($\beta = -5.0$, $P = .32$; $\beta = 0.6$, $P = .79$; $\beta = 7.4$, $P = .15$, respectively). Brain volume was significantly correlated with twins ($\beta = -77.2$, $P = .007$) (Online Supplemental Data).

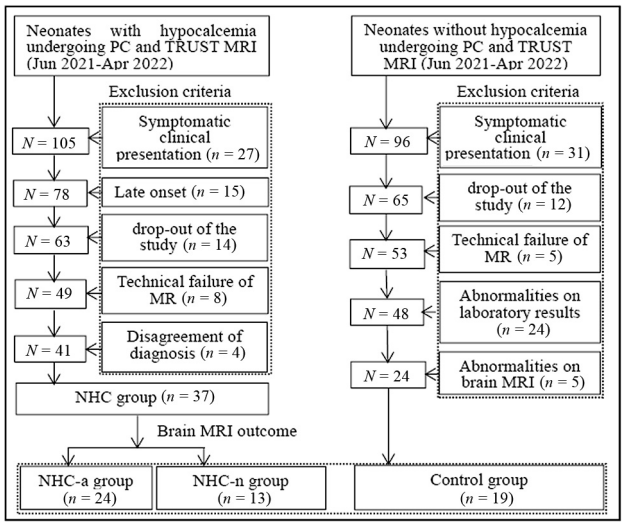

FIG 2. Flow chart of study participants.

Linear Regression Analysis of Measured Physiologic Parameters Associated with iCa Levels, Scan Age, Birth Weight, and Twins

Multilinear regression analysis showed that CBF and $CMRO_2$ demonstrated significant increases with iCa levels ($\beta = 8.2$, $P = .01$; $\beta = 24.2$, $P = .003$, respectively). Yv and brain volume were not dependent on iCa levels ($\beta = 2.0$, $P = .79$; $\beta = -7.8$, $P = .85$). Brain volume significantly correlated with twins ($\beta = -70.1$, $P = .01$) (Online Supplemental Data).

Logistic Regression Analysis of Measured Physiologic Parameters, Brain Volume, and iCa Levels to Detect NHC with Brain Injuries

The ORs were 0.80 (95% CI, 0.65–0.99) and 0.97 (95% CI, 0.89–1.05) for CBF and $CMRO_2$, respectively. The combined values together versus single values (CBF, $CMRO_2$, brain volume, or iCa levels, respectively) showed a superior capacity to detect NHC with brain injuries (area under curve [AUC] = 0.92 [95% CI, 0.83–0.99]) versus CBF (AUC = 0.82 [95% CI, 0.69–0.96]; $P = .001$), $CMRO_2$ (AUC = 0.73 [95% CI, 0.56–0.90]; $P = .02$), brain volume (AUC = 0.52 [95% CI: 0.32–0.72]; $P = .82$), or iCa levels (AUC = 0.62 [95% CI, 0.44–0.80]; $P = .23$) in Fig 5. The cutoff values for CBF and $CMRO_2$ were 12.75 mL/100 g/min and 22.63 μmol/100 g/min, respectively. The sensitivities with 95% CIs of the combined values together, CBF, and $CMRO_2$ were 85.1% (60.8%–93.3%), 80.5% (53.6%–86.9%), and 79.6% (53.3%–86.9%), respectively. Specificities with 95% CIs were 80.0% (75.0%–99.0%), 76.7% (61.1%–84.5%), and 73.3% (69.2%–81.2%), respectively.

DISCUSSION

In general, patients with NHC with structural abnormalities had impaired hemodynamics and cerebral metabolism. CBF and $CMRO_2$ were correlated with iCa levels, and CBF may be useful in assessing the need for calcium supplementation in asymptomatic NHC to prevent brain injury.

Table 2: MR imaging findings between the NHC group and the NHC-a subset

Characteristics of Neonatal MR Imaging	NHC ($n = 37$)	NHC-a ($n = 24$)
Periventricular WM lesions I (No.) (%)	6 (16.2)	6 (25)
Periventricular WM lesions II		
+0 (No.) (%)	4 (10.8)	4 (16.7)
+ Intraventricular hemorrhage (No.) (%)	1 (2.7)	1 (4.2)
Periventricular white matter lesions III (No.) (%)	1 (2.7)	1 (4.2)
Periventricular white matter lesions IV (No.) (%)	7 (18.9)	7 (29.2)
SAH without parenchymal hemorrhagic lesions (No.) (%)	5 (13.5)	5 (20.8)

Calcium Levels in the Neonate

Serum calcium levels in neonates are high at birth because calcium readily crosses the placenta to the fetus via active transport during the third trimester. After delivery, the maternal transfer of calcium halts and neonates may experience NHC during the first few days of

life. Although NHC is frequently asymptomatic, this condition can be potentially life-threatening.[2] Treatment is controversial, and evidence of its benefits is lacking.[5]

Effect of NHC on Physiologic Parameters and Structural Damage

Within the brain microcirculation, parenchymal arterioles are fundamental regulators of CBF.[27,28] The tone of parenchymal arterioles within the brain is controlled by astrocytes, which synthesize and release prostaglandins and epoxyeicosatrienoic acid via cyclooxygenase-1 and epoxygenase P450, respectively, in a Ca^{2+}-dependent manner. Ca^{2+} is not only indispensable for physiologic activities but is also an important second messenger in cells. The resulting increase in astrocytic Ca^{2+} leads to the synthesis and release of these vasodilators, which cause the dilation of brain arterioles and increase CBF. In addition, Ca^{2+} inhibits the inward current of Na^{+}. When hypocalcemia occurs, the inward current of Na^{+} increases, the threshold of the action potential decreases, and depolarization occurs. Subsequently, the voltage-dependent Ca^{2+} channel is activated, and calcium concentration increases, leading to a contraction of vascular smooth-muscle cells and reduction in CBF. This result may explain why the NHC group had poorer hemodynamics.

In addition, Ca^{2+} within the presynaptic terminal is key for chemical synaptic transmission. When intercellular Ca^{2+} is reduced, neurotransmitter release is inhibited. A lower calcium level leads to diminished neural activity, thus lower oxygen need and lower $CMRO_2$.

However, this impairment in hemodynamics was more significant in the NHC-a subset but not in the NHC-n subset, compared with controls. This finding might be related to the autoregulation of CBF. CBF regulation in the neonatal brain is distinct from that of the fully matured brain. The preterm rate is relatively high in this cohort (75.6% in NHC and 63.2% in control group). Infants born prematurely have an anatomically incomplete and underdeveloped cerebral vasculature and cannot fully autoregulate.[29] Once their cerebrovascular autoregulation cannot fully compensate for the effect of hypocalcemia, the probability of brain injuries increases (Online Supplemental Data).

The NHC-a group with brain injury mainly included patients with SAH and PVWM lesions. During activation of the clotting mechanism after SAH, coagulation factor IV (Ca^{2+}) is consumed. When SAH or PVWM lesions are accompanied by cerebral edema, Ca^{2+} will flow into the cell, causing a marked overload of intracellular Ca^{2+}, further promoting hypocalcemia.

Although it is possible that other factors may contribute to both impaired hemodynamics and structural lesions, we were able to control for most of the confounding factors by excluding participants with severe diseases and including age, sex, birth weight, Apgar

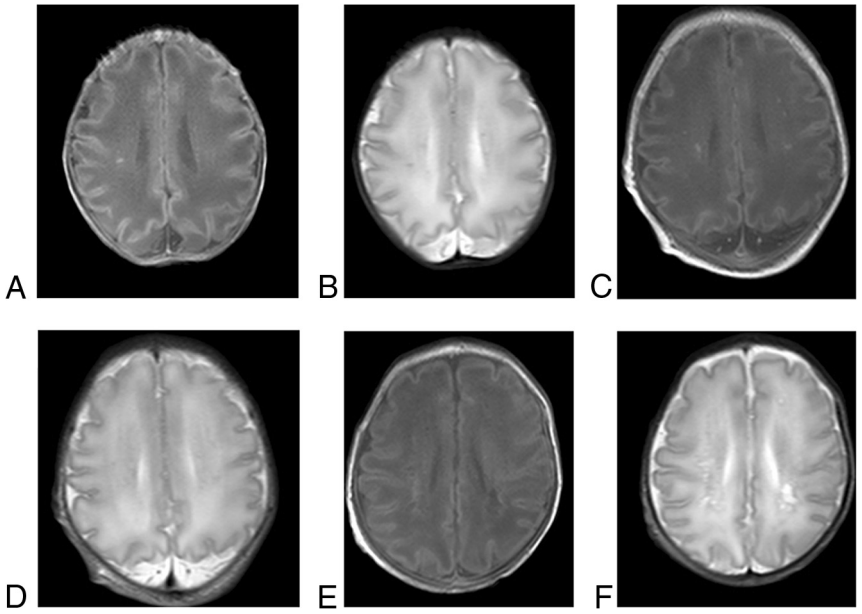

FIG 3. NHC-a subgroup with brain injuries on T1WI and T2WI. *A* and *B*, Neonate (scan age, 33.3 weeks; birth weight, 1740 g; male) had focal PVWM lesions (grade I) in the right PVWM area showing increased signal intensity on T1WI and decreased signal intensity on T2WI. *C* and *D*, Neonate (scan age, 34.3 weeks; birth weight, 2600 g; male) had PVWM lesions (grade II) in the bilateral PVWM areas, linearly displaying increased signal intensity on T1WI and decreased signal intensity on T2WI. *E* and *F*, Neonate (scan age, 37.7 weeks; birth weight, 2200 g; female) had clustered PVWM lesions and cystic lesions (grade IV) in bilateral PVWM areas.

Table 3: Comparison of physiologic parameters between groups and their subgroups ($n = 56$)[a]

Comparators	Yv (%)	CBF (mL/100g/min)	$CMRO_2$ (mL/100g/min)	Brain Volume (mL)
NHC group ($n = 37$)	63.4 (SD, 13.6)	13.3 (SD, 5.3)	31.1 (SD, 12.2)	300.0 (SD, 88.6)
Control group ($n = 19$)	64.7 (SD, 7.1)	16.5 (SD, 4.7)	40.4 (SD, 14.8)	290.4 (SD, 72.8)
P value	.64	<.05	<.05	.69
NHC-a group ($n = 24$)	63.2 (SD, 16.1)	11.2 (SD, 4.5)	27.4 (SD, 10.7)	296.9 (SD, 87.3)
NHC-n group ($n = 13$)	63.8 (SD, 7.5)	17.1 (SD, 4.7)	37.9 (SD, 12.1)	305.6 (SD, 94.2)
P value	.88	<.05	<.05	.78
NHC-a group ($n = 24$)	63.2 (SD, 16.1)	11.2 (SD, 4.5)	27.4 (SD, 10.7)	296.9 (SD, 87.3)
Control group ($n = 19$)	64.7 (SD, 7.1)	16.5 (SD, 4.7)	40.4 (SD, 14.8)	290.4 (SD, 72.8)
P value	.70	<.05	<.05	.80
NHC-n group ($n = 13$)	63.8 (SD, 7.5)	17.1 (SD, 4.7)	37.9 (SD, 12.1)	305.6 (SD, 94.2)
Control group ($n = 19$)	64.7 (SD, 7.1)	16.5 (SD, 4.7)	40.4 (SD, 14.8)	290.4 (SD, 72.8)
P value	.73	.70	.63	.61

[a] Data are expressed as means. *P* values are based on the Wilcoxon 2-sample exact test.

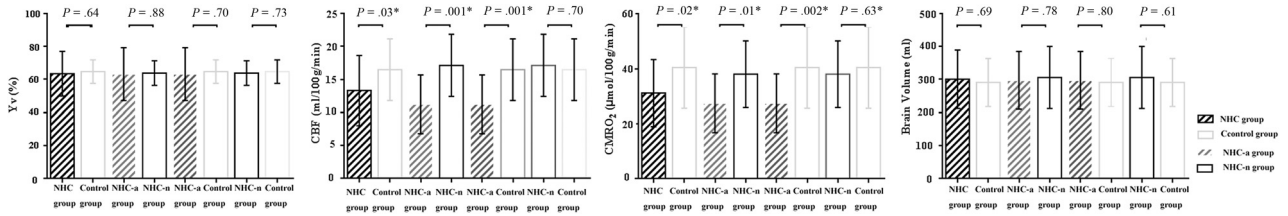

FIG 4. Boxplots of the physiologic parameters in both groups and subgroups. *A–D*, Boxplots display Yv, CBF, $CMRO_2$, and brain volume from both groups and subgroups. NHC neonates and the NHC-a subset (versus controls) both had significantly lower CBF ($P = .03$, $P = .001$) and $CMRO_2$ ($P = .02$, $P = .002$). CBF and $CMRO_2$ were significantly lower in NHC-a (versus the NHC-n) ($P = .001$, $P = .01$). There was no significant difference in CBF and $CMRO_2$ between those with NHC-n and controls ($P = .70$, $P = .63$). Yv and brain volume were not significantly different between groups ($P > .05$). The *asterisk* indicates $P < .05$.

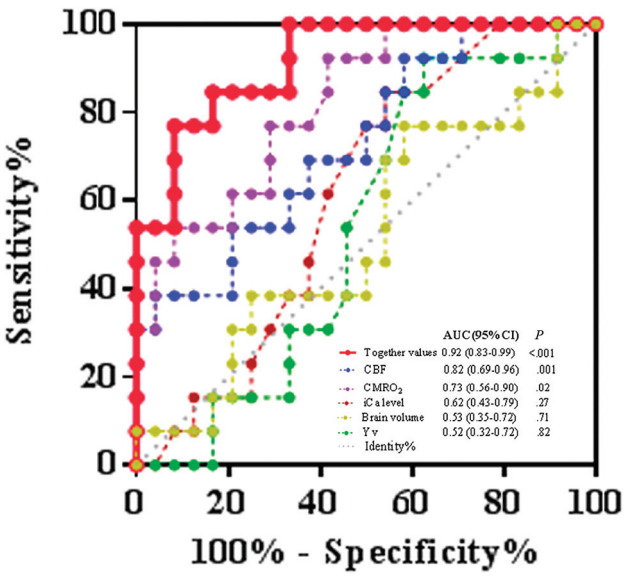

FIG 5. Receiver operating characteristic curve for the combined values together versus a single value (CBF, $CMRO_2$, brain volume, or iCa levels, respectively) to analyze the association between NHC and brain injuries. The combined values together versus a single value showed superior capacity to detect NHC with brain injuries (AUC= 0.92 [95% CI, 0.83-0.99]) versus CBF (AUC = 0.82 [95% CI, 0.69-0.96]; $P = .001$), $CMRO_2$ (AUC = 0.73 [95% CI, 0.56-0.90]; $P = .02$), brain volume (AUC = 0.53 [95% CI, 0.35-0.72]; $P = .82$), Yv (AUC = 0.52 [95% CI, 0.32-0.72]; $P = .82$), or iCa levels (AUC = 0.62 [95% CI, 0.44-0.80]; $P = .23$).

score, and blood gas analysis as covariates in multivariate regression analysis. Further studies with larger sample sizes and longitudinal follow-up are needed to better elucidate the causal relationship among calcium level, brain hemodynamics, and structure change.

Comparison with Previous Studies

Our measurements of Yv, CBF, and $CMRO_2$ in healthy neonates were comparable with those in previous reports,[21] demonstrating the accuracy and reliability of PCMR and TRUST MR imaging for assessing neonatal cerebral hemodynamics and metabolism.

There were limited reports on the cerebral hemodynamics and oxygen metabolism in NHC. CBF and $CMRO_2$ showed significant increases with iCa levels. The OR of NHC with brain injuries was 0.80 (95% CI, 0.65–0.99) for CBF. Thus, CBF may be a protective factor for asymptomatic NHC with brain injury. When a neonate with hypocalcemia has CBF of <12.75 mL/100 g/min (cutoff value), calcium supplementation might be considered to reduce the risk of brain injury.

Limitations

Our study has a moderate sample size. In future research, we will broaden the scope of our study to include follow-up of patients with NHC to clarify the impact of decreased CBF, $CMRO_2$, and iCa on neurocognitive deficits. In addition, SAH is negligible secondary to natural delivery. However, Wang et al[30] and Peng et al[31] reported that the myelin sheath was shown to be rapidly damaged and slowly recovered after SAH. Future studies for measurement of whether there are hemodynamic and metabolic abnormalities in neonates with SAH without parenchymal hemorrhagic lesions might be performed. There was 1 neonate with NRDS in grade III diagnosed by x-ray in our study who was administered a surfactant within 2 hours after birth. The administration of surfactant is performed by liquid bolus instillation into the endotracheal tube. Transient airway obstruction has been associated with rapid changes in oxygen saturation, heart rate, systemic blood pressure, and CBF. However, Terry et al[32] reported that CBF did not change significantly after surfactant administration. CBF that was not affected by fluctuations in arterial blood pressure during surfactant administration may indicate active autoregulation of flow by the cerebral vasculature. CBF remained unchanged until the mean arterial pressures fell below 35 mm Hg. In addition, MR dose not scan until neonate is stable. In our only case with NRDS grade III, an MR imaging examination was performed 7 days after birth, at which time the surfactant had little influence on CBF.

CONCLUSIONS

NHC with structural damage is likely to affect neonates with lower cerebral metabolism and hemodynamics. CBF may be useful in assessing the need for calcium supplementation in patients with asymptomatic NHC to prevent brain injury.

Disclosure forms provided by the authors are available with the full text and PDF of this article at www.ajnr.org.

REFERENCES

1. Moss CR. **Neonatal hypocalcemia in the infant of a diabetic mother.** *Neonatal Netw* 2020;39:200–04 CrossRef Medline

2. Cho WI, Yu HW, Chung HR, et al. **Clinical and laboratory characteristics of neonatal hypocalcemia.** *Ann Pediatr Endocrinol Metab* 2015;20:86–91 CrossRef Medline
3. Yilmaz B, Aygun C, Cetinoglu E. **Vitamin D levels in newborns and association with neonatal hypocalcemia.** *J Matern Fetal Neonatal Med* 2018;31:1889–93 CrossRef Medline
4. Levy-Shraga Y, Dallalzadeh K, Stern K, et al. **The many etiologies of neonatal hypocalcemic seizures.** *Pediatr Emerg Care* 2015;31:197–201 CrossRef Medline
5. Perino JM. **Calcium levels in the neonate.** *Neonatal Netw* 2020;39:35–39 CrossRef Medline
6. Kutilek S, Vracovska M, Pecenkova K, et al. **Calcemia and inflammatory markers in early-onset neonatal infection.** *Acta Medica (Hradec Kralove)* 2019;62:58–61 CrossRef Medline
7. Liu Y, Chai Y, Rong Z, et al. **Prognostic value of ionized calcium levels in neonatal sepsis.** *Ann Nutr Metab* 2020;76:193–200 CrossRef Medline
8. Wintermark M, Lepori D, Cotting J, et al. **Brain perfusion in children: evolution with age assessed by quantitative perfusion computed tomography.** *Pediatrics* 2004;113:1642–52 CrossRef Medline
9. Koziak AM, Winter J, Lee TY, et al. **Validation study of a pulsed arterial spin labeling technique by comparison to perfusion computed tomography.** *Magn Reson Imaging* 2008;26:543–53 CrossRef Medline
10. Wright EA, d'Esterre CD, Morrison LB, et al. **Absolute cerebral blood flow infarction threshold for 3-hour ischemia time determined with CT perfusion and 18F-FFMZ-PET imaging in a porcine model of cerebral ischemia**. *PLoS One* 2016;11:e0158157 CrossRef Medline
11. Pryds O, Greisen G, Skov LL, et al. **Carbon dioxide-related changes in cerebral blood volume and cerebral blood flow in mechanically ventilated preterm neonates: comparison of near infrared spectrophotometry and ^{133}xenon clearance.** *Pediatr Res* 1990;27:445–49 CrossRef Medline
12. Dallery F, Bouzerar R, Michel D, et al. **Perfusion magnetic resonance imaging in pediatric brain tumors.** *Neuroradiology* 2017;59:1143–53 CrossRef Medline
13. Diop M, Kishimoto J, Toronov V, et al. **Development of a combined broadband near-infrared and diffusion correlation system for monitoring cerebral blood flow and oxidative metabolism in preterm infants.** *Biomed Opt Express* 2015;6:3907–18 CrossRef Medline
14. Tortora D, Severino M, Rossi A. **Arterial spin labeling perfusion in neonates.** *Semin Fetal Neonatal Med* 2020;25:101130 CrossRef Medline
15. Ouyang M, Liu P, Jeon T, et al. **Heterogeneous increases of regional cerebral blood flow during preterm brain development: preliminary assessment with pseudo-continuous arterial spin labeled perfusion MRI.** *Neuroimage* 2017;147:233–42 CrossRef Medline
16. Liu P, Qi Y, Lin Z, et al. **Assessment of cerebral blood flow in neonates and infants: a phase-contrast MRI study.** *Neuroimage* 2019;185:926–33 CrossRef Medline
17. Ye FQ, Berman KF, Ellmore T, et al. **H(2)(15)O PET validation of steady-state arterial spin tagging cerebral blood flow measurements in humans.** *Magn Reson Med* 2000;44:450–56 CrossRef Medline
18. Armitage PA, Skipper N, Connolly DJ, et al. **A qualitative comparison of arterial spin labelling and dynamic susceptibility contrast MRI in 52 children with a range of neurological conditions.** *Br J Radiol* 2017;90:20160495 CrossRef Medline
19. van Osch MJ, Teeuwisse WM, van Walderveen MA, et al. **Can arterial spin labeling detect white matter perfusion signal?** *Magn Reson Med* 2009;62:165–73 CrossRef Medline
20. Qi Y, Liu P, Lin Z, et al. **Hemodynamic and metabolic assessment of neonates with punctate white matter lesions using phase-contrast MRI and T2-relaxation-under-spin-tagging (TRUST) MRI.** *Front Physiol* 2018;9:233 CrossRef Medline
21. Liu P, Huang H, Rollins N, et al. **Quantitative assessment of global cerebral metabolic rate of oxygen (CMRO2) in neonates using MRI.** *NMR Biomed* 2014;27:332–40 CrossRef Medline
22. Shetty AN, Lucke AM, Liu P, et al. **Cerebral oxygen metabolism during and after therapeutic hypothermia in neonatal hypoxic-ischemic encephalopathy: a feasibility study using magnetic resonance imaging.** *Pediatr Radiol* 2019;49:224–33 CrossRef Medline
23. Qi Y, Wang X, Mao J. **Quantitative assessment of cerebral metabolism and hemodynamics in small-for-gestational-age (SGA) newborns.** *Quant Imaging Med Surg* 2021;11:2321–32 CrossRef Medline
24. Wintermark P, Hansen A, Warfield SK, et al. **Near-infrared spectroscopy versus magnetic resonance imaging to study brain perfusion in newborns with hypoxic-ischemic encephalopathy treated with hypothermia.** *Neuroimage* 2014;85(Pt 1):287–93 CrossRef Medline
25. Childs AM, Cornette L, Ramenghi LA, et al. **Magnetic resonance and cranial ultrasound characteristics of periventricular white matter abnormalities in newborn infants.** *Clin Radiol* 2001;56:647–55 CrossRef Medline
26. Herscovitch P, Mintun MA, Raichle ME. **Brain oxygen utilization measured with oxygen-15 radiotracers and positron emission tomography: generation of metabolic images.** *J Nucl Med* 1985;26:416–17 Medline
27. Elsary AY, Elgameel AA, Mohammed WS, et al. **Neonatal hypocalcemia and its relation to vitamin D and calcium supplementation.** *Saudi Med J* 2018;39:247–53 CrossRef Medline
28. Dabertrand F, Nelson MT, Brayden JE. **Ryanodine receptors, calcium signaling, and regulation of vascular tone in the cerebral parenchymal microcirculation.** *Microcirculation* 2013;20:307–16 CrossRef Medline
29. Rhee CJ, da Costa CS, Austin T, et al. **Neonatal cerebrovascular autoregulation.** *Pediatr Res* 2018;84:602–10 CrossRef Medline
30. Wang Y, Xu J, You W, et al. **Roles of Rufy3 in experimental subarachnoid hemorrhage-induced early brain injury via accelerating neuronal axon repair and synaptic plasticity.** *Mol Brain* 2022;15:35 CrossRef Medline
31. Peng J, Pang J, Huang L, et al. **LRP1 activation attenuates white matter injury by modulating microglial polarization through Shc1/PI3K/Akt pathway after subarachnoid hemorrhage in rats.** *Redox Biol* 2019;21:101121 CrossRef Medline
32. Terry MH, Merritt TA, Harding B, et al. **Pulmonary distribution of lucinactant and poractant alfa and their peridosing hemodynamic effects in a preterm lamb model of respiratory distress syndrome.** *Pediatr Res* 2010;68:193–98 CrossRefMedline